Received March 24, 2019, accepted April 9, 2019, date of publication April 24, 2019, date of current version May 14, 2019.

Digital Object Identifier 10.1109/ACCESS.2019.2912548

Secure EEG Signal Transmission for Remote Health Monitoring Using Optical Chaos

ROMANA SHAHZADI[1], SYED MUHAMMAD ANWAR[1,2], FARHAN QAMAR[1], MUDASSAR ALI[1], JOEL J. P. C. RODRIGUES[3,4,5], (Senior Member, IEEE), AND MAJDI ALNOWAMI[6]

[1]Department of Telecommunication and Information Engineering, University of Engineering and Technology, Taxila 47050, Pakistan
[2]Center of Research in Computer Vision, The University of Central Florida, Orlando, FL 32816, USA
[3]National Institute of Telecommunications (Inatel), Santa Rita do Sapucaí 37540-000, Brazil
[4]Instituto de Telecomunicações, 1049-001 Lisbon, Portugal
[5]PPGEE, Federal University of Piauí, Campus Ministro Petrônio Portella, Teresina 64049-550, Brazil
[6]Medical Physics Group, Department of Nuclear Engineering, King Abdulaziz University, Jeddah 21589, Saudi Arabia

Corresponding authors: Romana Shahzadi (romana.farhan@uettaxila.edu.pk) and Syed Muhammad Anwar (s.anwar@uettaxila.edu.pk)

ABSTRACT For the very first time, we present the use of optical chaos for the secure transmission of electroencephalogram (EEG) signals through optical fiber medium in remote health monitoring systems. In our proposed scheme, a semiconductor laser source is used to generate optical chaos, which hides EEG signal before its transmission over the optical fiber medium. The EEG signals are acquired by using a 14-channel Emotiv headset device, which are then processed and rescaled to be compatible with the experimental environment (Optisystem). The mixing of EEG signals and chaos is performed using additive chaos masking scheme, which exhibits certain useful properties such as simplicity and easy recovery of the message. Chaotic data (a combination of EEG signals and chaos) is sent over the optical fiber medium to investigate propagation issues associated with secure EEG signal transmission. The scheme is implemented for long haul communication in which the linear impairments of optical fiber are controlled for successful transmission of the secure signal. The parameters at transmitting and receiving sides are selected to achieve synchronization, such that the transmitted signal could be subtracted from identical chaos to restore the original EEG signal at the receiving side. The scheme is tested for different lengths of the optical fiber cable in which the quality of the received signal is determined by obtaining Q-factors. This scheme could also be used with medical signals such as electrocardiography and electromyography.

INDEX TERMS EEG signal, Emotiv, semiconductor laser, optical chaos, additive chaos masking, synchronization, remote health monitoring, long haul.

I. INTRODUCTION

Electroencephalogram (EEG) reflects the electrical activity of the brain that can be used to detect brain disorders. This electrical activity consists of distinct frequency ranges, which define various characteristics of the underlying brain function [1]. The cortical nerve cell inhibitory and excitatory postsynaptic potentials produce EEG signals. These postsynaptic potentials summate in the cortex and reach surface of the scalp where they are recorded as EEG [2]. The EEG signals can be recorded by placing electrodes on a patient's head region at the scalp [3]. Hence, they can be used non-invasively to detect brain function as well as disorders such as head injury, brain tumor, memory problems, stroke, encephalitis, brain dysfunction, sleep disorder, and dementia. In addition, EEG signals can also be used to detect mood and emotions [4]–[6]. However, these waveforms can only be interpreted by a trained neurophysiologist whose presence may not be ensured at all places particularly in remote locations i.e., clinics and hospitals. Thus, EEG signals transmission to places, where a trained neurophysiologist is present, has become a critical need of time in order to have an accurate and timely treatment of patients suffering from serious brain disorders. However, patient data consists of highly sensitive information that must be transmitted in such a way that no one can eavesdrop or change the contents. So, to implement the concept of e-health monitoring in its true spirit, the security of the underlying patient's data is one of the key concerns [7].

The associate editor coordinating the review of this manuscript and approving it for publication was Pallab K. Choudhury.

Traditionally, remote health monitoring using EEG signals was carried out by using telephonic lines based on copper wire networks [8]. However, this approach is not suitable for long distance transmission due to high telephonic charges, huge signal power loss and addition of various noises. The additional security features on patient's data cost extra bandwidth which results in total failure of these traditional networks. Optical fiber cable has become an optimal choice for medical data transmission due to its high bandwidth, long distance transmission capability, and minimum noise interference [9]. Another major advantage is improved security, since chaos based optical communication systems offer excellent security features compared to traditional cryptographic schemes.

Due to flexible digital signal processing, ease in key management, and reduced implementation complexity, the physical layer holds an edge on upper layers in the Open System Interconnection (OSI) model [10], [11]. The physical layer chaos-based communication can be divided into two categories. The first one includes encryption of data in the optical domain such as chaotic laser communication, exclusive OR scrambling, optical key distribution, and optical steganography [12]. The second one deals with the encryption of data in electrical domain such as piecewise chaotic permutation and fractional Fourier transform. The drawbacks of encryption in optical domain includes limitations in key distribution, high sensitivity problems, and small space for key encryption. In electrical domain encryption, high randomness of chaotic sequences is limited by finite accuracy of computer [13].

Major applications of optical chaos include secure communication [14], [15], random number generation [16], [17], wideband signal generation [18], [19], chaotic ladar [20], [21], optical time domain reflectometer (OTDR) [22], [23], remote/sensor radar [24], [25] and image encryption [26], [27]. Based on the transmission medium, secure communication through optical chaos can be further divided into two types, including optical fiber communication [28] and wireless communication such as free space optics (FSO) or optical wireless communications (OWC) [29], [30].

In optical communication system, message can be hided inside chaos by three different ways i.e. additive chaos masking (ACM), chaos shift keying (CSK) and chaos modulation (CM) [31], [32]. These three different schemes have their own pros and cons however, ACM is chosen in our proposed model due to its simplicity, easy recovery of message and implementation in Optisystem software v14.0.

Our proposed security implementation through ACM scheme is shown in Fig. 1, where two similar chaotic systems are deployed both at the transmitting and receiving sides. The original data signal (d(t)) is masked with the chaotic signal (c(t)) generated by one chaotic laser deployed at the transmitting side to generate a secure signal (s(t)) before its transmission over the optical fiber channel. To generate optical chaos through chaotic laser, we use direct modulation method in which a current source is directly attached to the semiconductor laser. The parameters of the current source

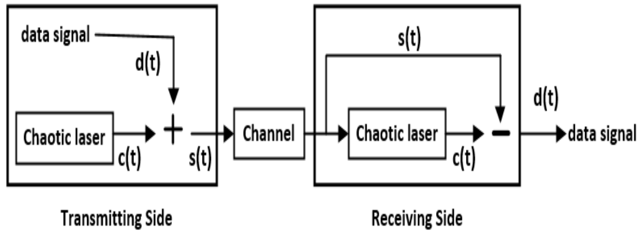

FIGURE 1. Additive chaos masking.

and semiconductor laser are controlled to produce chaos with desired attributes. This signal (s(t)) acts as a noise for intruders and contains the hidden original data (d(t)). The signal (s(t)) is then transmitted over the channel and is subtracted by a similar chaotic signal (c(t)), but this time generated by a second chaotic semiconductor laser deployed at the receiving side. All parameters of the second chaotic laser are kept like the transmitting laser so that subtraction rule could be applied to retrieve the original data (d(t)). In addition to similar parameters for both the chaotic lasers, another important task is to achieve synchronization between these chaotic lasers. A tiny mismatch between these lasers can result in total failure of this scheme. We have used ACM scheme for the EEG signals, which critically requires perfect synchronization because of the inherent low strength.

Our major contributions are as follows,

1. To the best of our knowledge, this is for the first time that EEG signals are secured by applying ACM scheme for transmission over an optical fiber cable.
2. Preprocessed EEG signals are obtained by using EMOTIV headset along with the SDK kit v.3.3.3 These signals are rescaled to make them compatible with the Optisystem environment.
3. We present a step by step approach starting from EEG signal acquisition, preprocessing, effects of optical fiber channel on chaos hiding EEG signal and the retrieval of original EEG signal from chaos.

This paper is organized in following sections. Section-I covers introduction of paper. Section-II presents the mathematical model and operating parameters. Section-III comprises of the proposed setup for simulations. Section-IV consists of results and discussions. Finally, the conclusions are presented in Section-V.

II. MATHEMATICAL MODEL

Chaos based optical communication system requires the same chaos at both the transmitting and receiving sides. The existing literature has reported two types of chaotic waveforms. Non-pulsating chaos can be produced either by Erbium doped fiber ring laser (EDFRL) arrangements based on nonlinearities or through continuous oscillations produced by semiconductor lasers [33]. Whereas, pulsating chaos can be generated by either modulating the semiconductor lasers or through pump or cavity loss of modulated EDFRLs [34]. The phenomenon behind pulsating chaos is the occurrence of population inversion state for specific time and then instant release of energy in the form of chaotic pulse. As the energy stored during population inversion is not fully consumed in a single cycle, the remaining energy acts as a starting point for the next buildup of new pulse and hence the amplitude of every chaotic pulse becomes different. More randomness can be seen in the behavior if the chaotic pulses are not fired at the fixed time. For pulsating chaos, the amplitude of every consecutive optical pulse touches zero value. The shape of these pulses is Gaussian in nature, which can be checked by applying a Gaussian fit [34]. Pulsating chaos can be further classified into two parts i.e., pulsating chaos with random amplitude but fixed time interval and pulsating chaos having random amplitude and random time interval. The later one is more indeterministic and chosen for our proposed setup to offer better security.

Moreover, security analysis in the proposed chaos-based communication system is done by using the Lyapunov exponents. Larger the values of Lyapunov exponents along the positive side indicates greater security in the communication system [33], [35]. As pulsating chaos shows greater values of Lyapunov exponent along positive side, thus offers better security than non-pulsating chaos [36]. A higher degree of chaos is achieved by performing direct modulation of the semiconductor laser.

In direct modulation technique, a current source is directly connected with semiconductor laser whose parameters (current and frequency) are controlled to generate the chaotic waveform of required bandwidth and amplitude. The chaos produced in this way is highly indeterministic and of high bandwidth, which can be effectively used for securing signals with a higher data rate. Optical chaos generated by semiconductor laser can be represented by the following laser rate equations [37],

$$\frac{dn}{dt} = \frac{J}{ed} - G(n)S - \frac{n}{\tau_n} \tag{1}$$

$$\frac{dS}{dt} = G(n)S - \frac{s}{\tau_{ph}} + \beta_{sp}\frac{n}{\tau_r} \tag{2}$$

In Eq (1), 'n' is the concentration of carrier, 'J' is the injection current density (in active layer it is electric current flowing per unit area), 'e' represents the elementary charge, 'd' is the thickness of active layer. '$G(n)$' defines the mode amplification rate due to stimulated emission & 'τ_n' is carrier lifetime. Whereas in Eq (2), 'S' is photon density, 'τ_{ph}' represents photon lifetime, 'β_{sp}' defines coupling factor due to spontaneous emission and 'τ_r' is the radiative recombination lifetime due to the spontaneous emission. Eq.1 can be written as,

$$\frac{dn}{dt} = \frac{d\left(N/V_a\right)}{dt} = \frac{1}{V_a}\frac{dN}{dt} \tag{3}$$

where $n = N/V_a$ and 'N' is the number of carriers in active layer. 'V_a' is the volume of active layer. By solving Eq. 3

$$= \frac{1}{V_a}\left[\frac{l}{e} - g(n)\Gamma_a N_{ph} - \frac{N}{\tau_n}\right] \tag{4}$$

In Eq (4), 'I' is the injection current that is flowing through the active layer. 'N_{ph}' are the number of photons. '$g(n)$' represents the amplification rate due to the stimulated emission in the active layer.

$$= \frac{\mathrm{I}/V_a}{e} - g(n)\frac{V_a}{V_m}\frac{N_{ph}}{V_a} - \frac{\mathrm{N}/V_a}{\tau_n} \tag{5}$$

where, $\Gamma = \mathrm{V_a/V_m}$.

By solving Eq (5),

$$= \frac{J}{ed} - g(n)s - \frac{n}{\tau_n} \tag{6}$$

Now, modifying Eq (2),

$$\frac{ds}{dt} = \frac{d\left(N_{ph}/V_m\right)}{dt} = \frac{1}{V_m}\frac{dN_{ph}}{dt} \tag{7}$$

$$= \frac{1}{v_m}\left[g(n)\Gamma_a N_{ph} - \frac{N_{ph}}{\tau_{ph}} + \beta_{sp}\frac{N}{\tau_r}\right] \tag{8}$$

$$= g(n)\Gamma_a\frac{N_{ph}}{V_m} - \frac{N_{ph}/V_m}{\tau_{ph}} + \beta_{sp}\frac{N/V_m}{\tau_r} \tag{9}$$

$$= g(n)s\Gamma_a - \frac{s}{\tau_{ph}} + \Gamma_a\beta_{sp}\frac{n}{\tau_r} \tag{10}$$

Eq (6) and Eq (10) are the required solved rate equations for producing chaos through semiconductor lasers. Parameters and their values which are used in our setup to control chaos are given in Table 1 and Table 2.

TABLE 1. Chaotic laser (physical parameters).

Symbol	Physical Parameters	Value
β_{sp}	Fraction of spontaneous emission coupled into the lasing mode	8×10^{-7}
V_a	Active Layer Volume	1.55×10^{-10}
Γ_a	Mode confinement factor	0.42
τ_n	Electron lifetime	1.3×10^{-9}
τ_{ph}	Photon lifetime	3.1×10^{-12}
Λ	Linewidth Enhancement Factor	4
N	Carrier density at transparency	1×10^{18}

TABLE 2. Chaotic laser (operating parameters).

Parameter	Values
Power	0-10 dBm
Wavelength	1550 nm
Threshold power	0.140 mW
Bias Current	32 mA
Modulation Peak Current	37 mA
Threshold Current	34 mA
Power at Bias Current	0 dBm

III. OUR PROPOSED SCHEME

EEG signals were acquired by using Emotiv EEG head set which is commercially available along with its premium software development kit (SDK version 3.3.3, San Francisco-USA) and shown in Fig. 2. This headset provides EEG signal

FIGURE 2. Emotiv headset used for EEG signal acquisition.

recording by using 14 electrodes positioned according to the 10/20 electrode positioning system (Fig. 3). The right and left hemispheres are served by two more electrodes which act as reference electrodes. In order to reduce the resistance between the skull and electrodes, saline liquid is utilized.

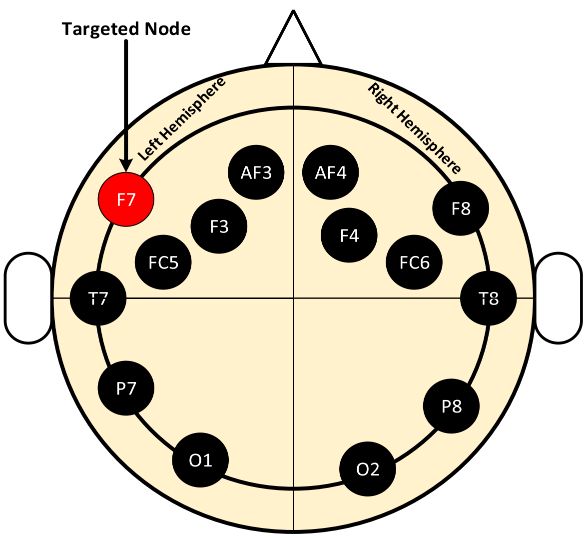

FIGURE 3. 10-20 electrode positioning for EEG signal collection through EMOTIV headset.

The recorded brain signals were transferred to a computer system having the EMOTIV SDK software. The headset was connected to the computer system over Bluetooth interface via a proprietary dongle connected to the USB port. For data acquisition, the EEG headset was placed on head of a person sitting in a room with comfortable environment and minimum noise sources. Noise sources such as electrical lines, movement of electrodes, and mobile phone signals were avoided. The headset was synchronized with SDK kit for acquiring and transferring data to the desktop system without errors. Although, the EEG data was acquired in a noise free environment, but the signals are affected by impairments due to movement of the person and equipment such as heartbeat, sweating, muscular movement, eye-blinks and movement of electrodes etc. The noises added due to these unavoidable effects significantly reduce the quality of the EEG signals required for clinical analysis and interpretation. The average range of the amplitude of an EEG signal lies between $20 - 50\ \mu$ V and bandwidth of $0.2 - 100$ Hz. The EEG signal in our proposed setup is recorded at a rate of 128 samples/sec.

For removing impairments in the recorded signal, different measures were taken in the preprocessing stage. The DC offset was removed by subtracting mean values from the complete data. Filtering and independent component analysis (ICA), was used for the purpose of noise removal from the EEG signal. Muscular movements responsible for degrading the EEG signals above 45 Hz were removed by using the Butterworth's filter with a band-pass of 5-45 Hz. The filtering process also helped to remove the power line interference at 50 Hz caused by electrical wires. Among the 14 electrodes, we selected F7 channel to implement the security features.

In our proposed scheme for the security of EEG signals through optical chaos (Fig. 4) the pre-processed EEG signal was fed into Mach-Zehnder modulator (MZM). It modulates electrical EEG signal with the beam of light produced by a continuous wave (CW) laser. The wavelength of CW laser was set to 1552 nm so that the EEG signal could be sent with less attenuation loss as supported by the optical fiber channel at this wavelength. The extinction ratio of MZM, which is defined as the ratio of two optical power levels of a digital signal generated by laser, was set to 50:50 to support the modulation of EEG signal with the laser light. The optical output of MZM was then given to the optical adder, where this waveform was mixed with optical chaos produced by the chaotic semiconductor laser. The operating wavelength of the chaotic semiconductor laser was kept around 1552 nm, which allowed mixing of two waveforms properly i.e., chaos generated by semiconductor laser and light produced by the CW laser modulating EEG waveform.

The output of the optical adder which is now a secure EEG signal in optical domain, was sent over a single mode fiber. To check the feasibility of our proposed scheme for longer distances, three different fiber lengths i.e., 5 km, 80 km and 120 km were evaluated in the experimental setup for signal transmission. As the signal power drop is 0.2 dB/km in single mode optical fiber, the gain of optical amplifier was set accordingly to compensate the attenuation for different lengths of optical fiber. For this purpose, an optical link amplifier (OLA) was used in the post order configuration in which it was deployed just after the optical fiber cable. In addition to attenuation losses, another linear impairment which plays a significant role in signal distortion is the dispersion effect. Dispersion causes the broadening of pulses in time domain, which further leads to inter-symbol interference due to overlapping of pulses, resulting in an overall degradation of signal quality. In order to control the dispersion, dispersion compensation fiber (DCF) was used in the post order configuration, whose value was set to -16.75 ps/nm/km to eliminate dispersion effects for different fiber lengths.

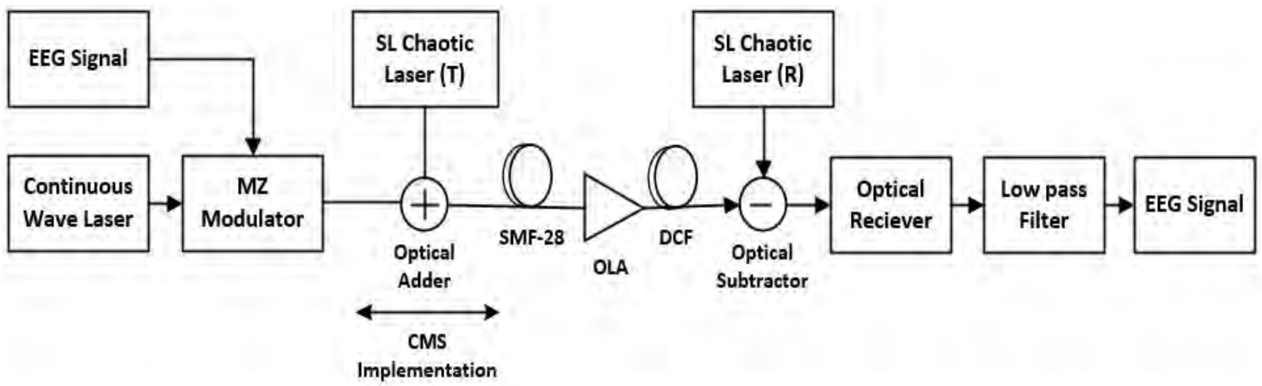

FIGURE 4. Our proposed scheme for adding chaos to the EEG signals.

At the receiving side, before signal detection at the photodiode or optical receiver, the signal was subtracted from an identical chaos generated by the second semiconductor laser deployed at the receiving side. The operating parameters of both these semiconductor lasers were controlled in such a way that identical chaos was produced at both sides. After performing subtraction through optical subtractor, the signal was detected at optical receiver, whose function was to convert the signal from optical to electrical domain. Avalanche photodiode (APD) was used due to its high sensitivity and capability to detect low power signal. The signal was then passed through a low pass filter to further eliminate noise effects and recover the original EEG signal.

Since our proposed scheme for EEG signal encryption is chaos based, it is highly sensitive to the initial conditions [38], [39] and perfect synchronization is required between transmitter and receiver. A little mismatch between the transmitter and receiver parameters can lead to complete failure. Secondly, EEG waveform exhibits important features at each point of waveform and a minute deviation in the received signal can lead to misinterpretation.

IV. RESULTS AND DISCUSSION

Emotiv EEG headset was used to record the brain activity at electrode positions F3, AF3, F7, P7, T7, FC5, O1, F4, AF4, F8, P8, T8, FC6 and O2. Among these, signals recorded at F7 (Fig. 5) electrode were chosen in our proposed setup for security implementation through optical chaos. Although, the selection was made due to strong signal strength, our proposed scheme is valid for all other channels as well. The plotted raw signal shows the amplitude values (microvolts) along y-axis and the number of samples along x-axis and includes various types of noises which are eliminated by performing preprocessing as discussed in section-III.

The signal after performing preprocessing and rescaling is shown in Fig. 6. The preprocessing stage eliminates various noises from the raw signal whereas rescaling is done to make F7 EEG signal compatible with the Optisystem environment. In the rescaling step, y-axis values of the signal are changed to milliwatts (mW), whereas x-axis values are changed to nanoseconds (ns). Now, this signal is compatible with the Optisystem environment where different operations can be performed for security implementation and analysis of secure

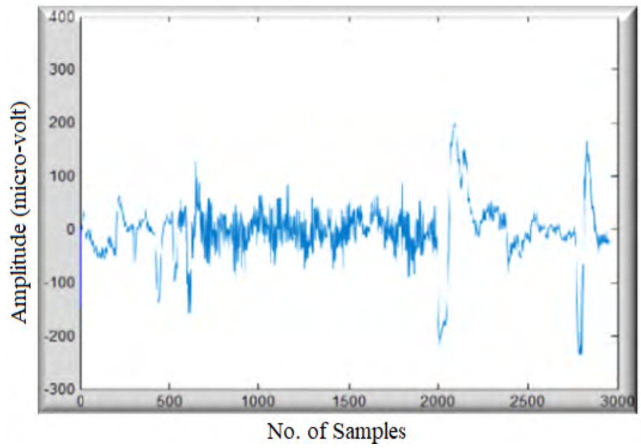

FIGURE 5. F7 EEG signal (raw form) acquired by using Emotiv EEG headset.

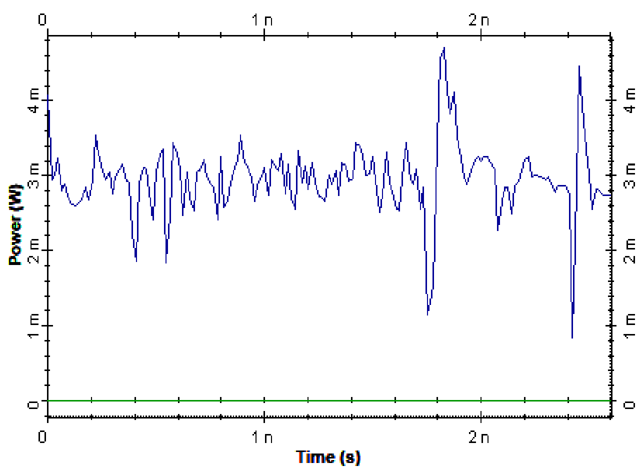

FIGURE 6. EEG signal imported in Optisystem environment after eliminating noises.

signal propagation in optical fiber medium for long distance transmission.

The high bandwidth chaos produced by using semiconductor laser (Fig. 7) can easily hide EEG pulses within itself. For chaotic communication, the recommended bandwidth of chaos is ten times the bandwidth of the signal which needs to be secured. As the communication is on optical fiber channel so bandwidth is not an issue for security implementation in our proposed scheme. The parameters of semiconductor lasers were controlled to generate chaotic pulses of the required amplitude for EEG signal encryption.

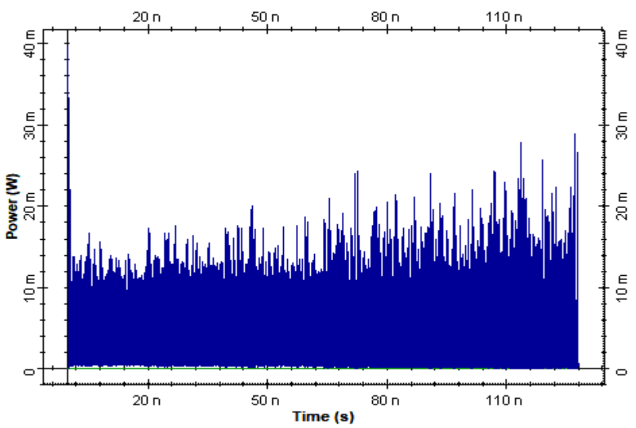

FIGURE 7. Chaos produced through semiconductor laser.

A zoomed plot (Fig. 8) of chaotic pulses (Fig. 7) shows the randomness of these pulses in amplitude and follow the Gaussian curve. The shape of these pulses can be represented by the following equation,

$$E_{LA} = \frac{A_n e^{-(t-t_n)^2/2\delta^2}}{\delta\sqrt{2\pi}} \quad (11)$$

where, 'A_n' represents the amplitude scaling, 'δ' shows the standard deviation, 't' indicates time and 't_n' denotes time instance of nth chaotic pulse. 'Gain quenching' which is another important parameter of chaotic pulses can also be

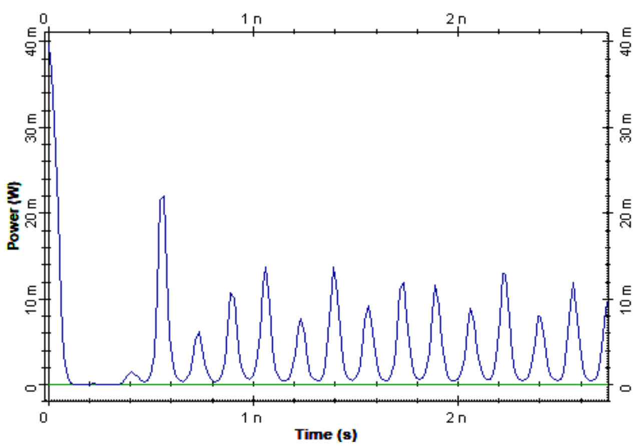

FIGURE 8. A zoomed plot of the chaos signal.

seen in Fig. 8, where high and low amplitude pulses are followed by each other.

The EEG signal (Fig. 6) was modulated with the CW laser light to send it over the optical fiber medium. However, for security implementation this signal was mixed with chaotic waveform (Fig. 8). This mixing was done by using the optical adder. Fig. 9 is a noise like signal, which cannot be read by an intruder at any point between the transmitter and receiver.

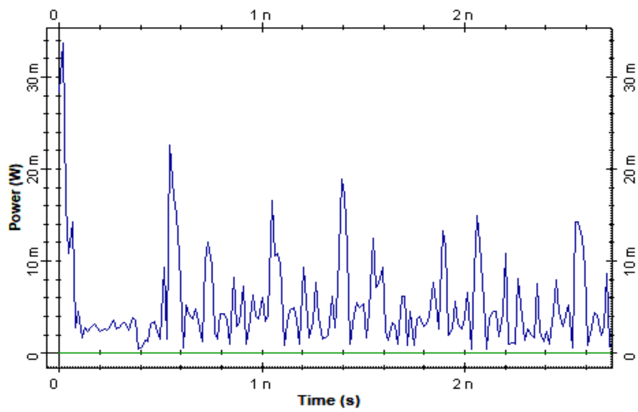

FIGURE 9. Optical chaos hiding EEG signal.

The security of EEG signal is evident from time domain plot (Fig. 9), however it is equally important to analyze the signal's security in frequency domain. Fig. 10. shows the optical spectrum of EEG signal with frequency centered at 193.1Thz before adding chaos. Whereas, Fig. 11 shows the change in spectrum when chaos is added in the original EEG signal. The altered spectrum shows that it is now impossible to read the signal in frequency domain as well. It is important to note that both the spectrums are centered at the same frequencies which is essential for proper mixing of signals. Time domain plots are taken by using optical time domain visualizers (OTDV), whereas signals in frequency domain are observed by using optical spectrum analyzers (OSA).

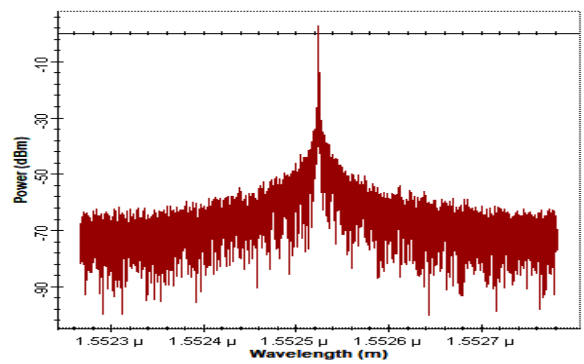

FIGURE 10. Optical spectrum of CW laser modulating EEG signal at 193.1 THz.

The propagation of chaos signal hiding the EEG signal was studied for long distance communication. First, the effects of linear impairments inside the optical fiber were analyzed

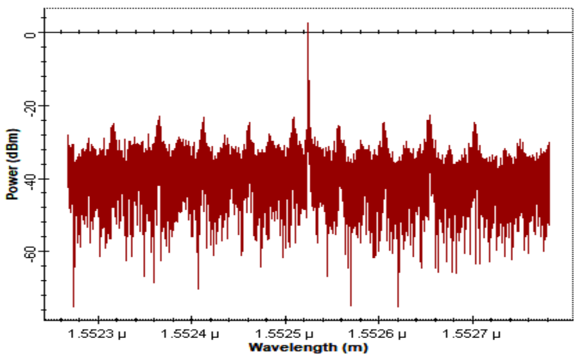

FIGURE 11. Optical spectrum of chaos hiding EEG signal.

at a distance of 5 km. These linear impairments involve attenuation and dispersion effects (Fig. 12) as seen in the overlaid plots of transmitted and received chaotic waveforms. It is evident that received pulses not only lost their peak powers but also get broaden in time domain. In addition, pulse shifting in time can also be observed.

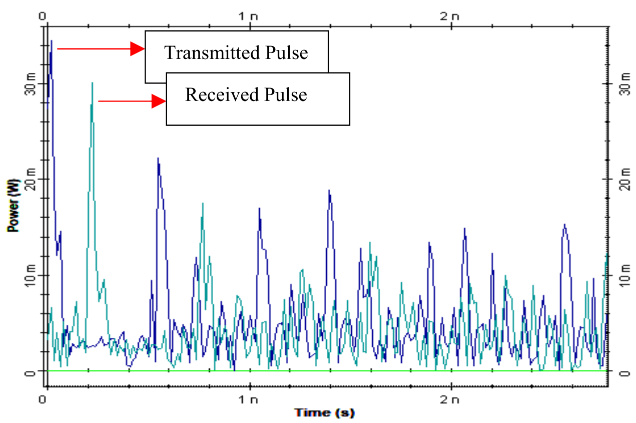

FIGURE 12. Transmitted vs received chaotic pulses at 5 km of fiber length without linear impairments control.

As the power drop in optical fiber is 0.2 dB/km so an optical amplifier with a total gain of 1.0 dB was used for the attenuation compensation for 5 km of fiber length. In order to control the dispersion of same fiber length, 1 km of DCF was used having a total value of −83.75 ps/nm/km. This value is 5 times the normal value of dispersion in optical fiber but in opposite direction so that the total dispersion of optical fiber cable was cancelled out. The transmitted received chaotic pulses exactly matched after controlling attenuation and dispersion (Fig. 13).

The deterioration of the received chaos with respect to the transmitted chaos is evident from the scatterplots (Fig. 14 and Fig. 15) before and after controlling the attenuation, dispersion, and link delays of optical fiber, respectively. The deviation (Fig. 14) clearly suggests a problematic transmission of chaotic signal.

At the receiving side, the chaotic signal containing F7 EEG signal was subtracted from the identical chaos produced by

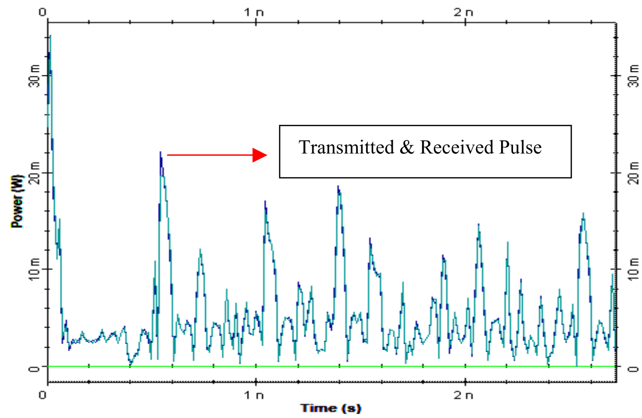

FIGURE 13. Transmitted vs received chaotic pulses at 5 km of fiber length after linear impairments control.

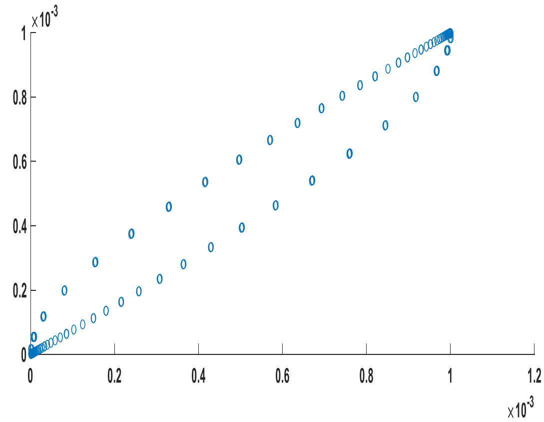

FIGURE 14. Scatterplot before controlling attenuation, dispersion and link delay.

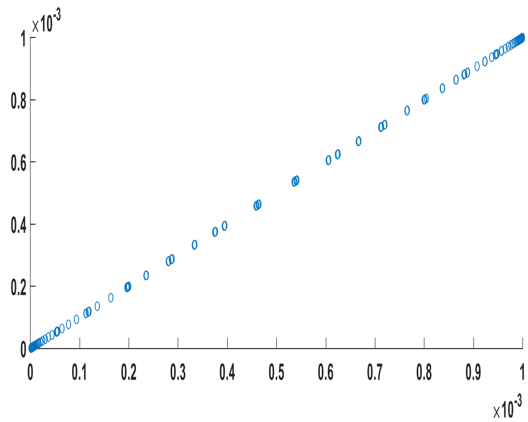

FIGURE 15. Scatterplot after controlling attenuation, dispersion and link delay.

the second semiconductor laser. The signal was detected by the photodiode which converted it into a signal like the original F7 EEG signal. A low pass filter was used to further refine the received signal. The original and decrypted EEG signals are shown in Fig. 16 (a) and (b) respectively. We measured the Q-factor (Fig. 17) of chaotic EEG signal for long haul

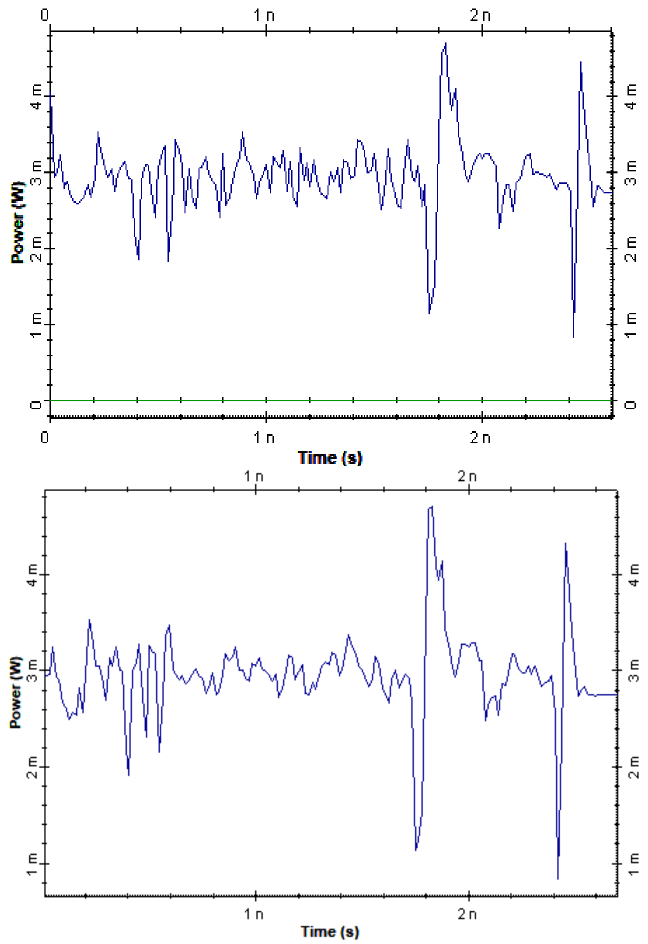

FIGURE 16. Transmitted EEG signal vs received EEG signal (a) original EEG (b) decrypted EEG signal.

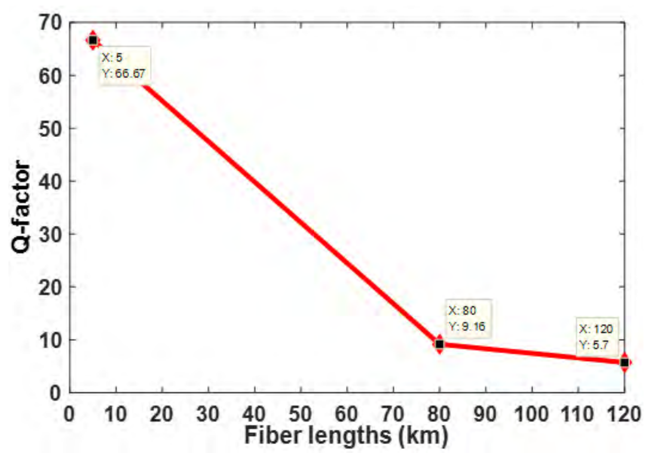

FIGURE 17. Q-factor vs optical fiber lengths.

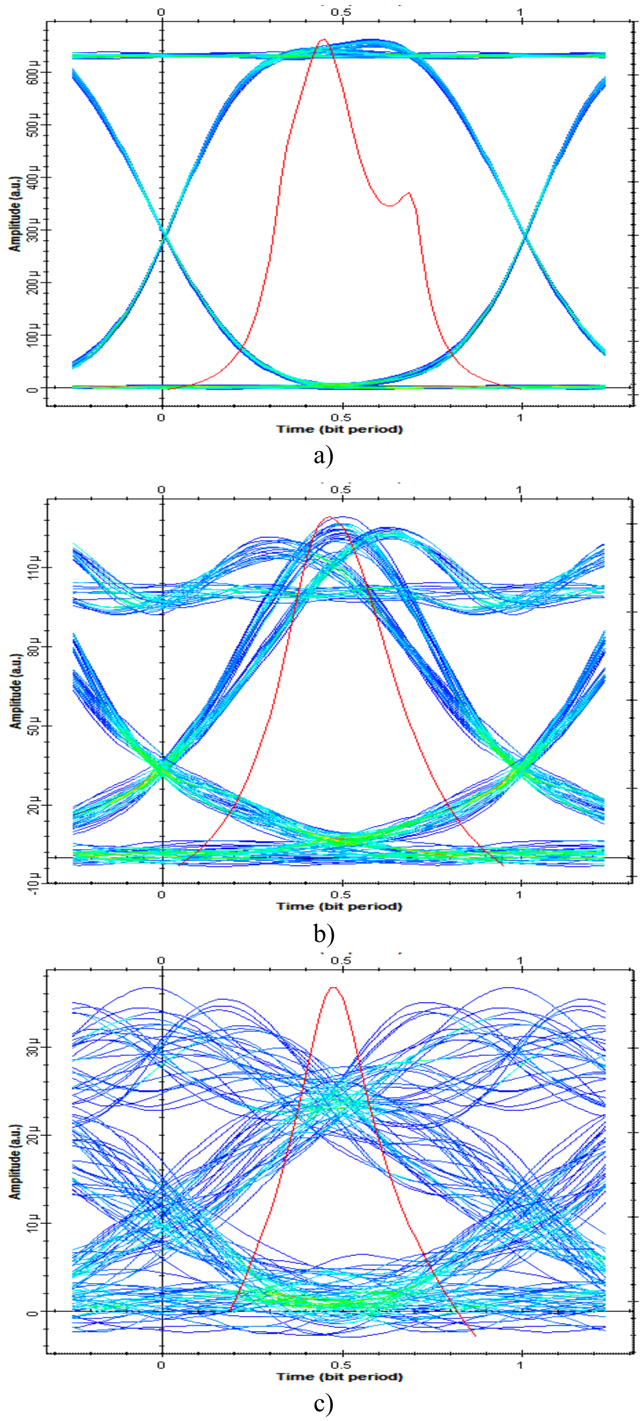

FIGURE 18. Eye-diagrams showing quality of received EEG signal at different fiber lengths.

transmission by transmitting the digital form of EEG signal over 5, 80 and 120 km of fiber lengths. We observed a drastic deterioration in Q-factor at greater fiber lengths.

From the eye-diagrams (Fig. 18), where red lines show the Q-factor directly proportional to the height of eye-opening, at 5 km (Fig. 18 (a)), 80 km (Fig. 18 (b)), and 120 km (Fig. 18 (c)) respectively, we can see that at 80 km (Q-factor is 9.16) the eye-opening is good enough for recovery of EEG signal in its exact form. However, reaching 120 km of fiber length, the eye-diagram is badly affected, and the Q-factor is dropped to 5.7, where it is almost impossible to recover the exact EEG signal from chaos at the receiving side.

V. CONCLUSION

We presented a method for secure transmission of EEG signals using ACM scheme for the first time to the best of our knowledge. EEG signals were recorded from the Emotiv EEG headset, preprocessed to eliminate noises and made compatible with the Optisystem environment after rescaling. Among different signals acquired through 14 different electrodes of Emotiv kit, F7 signal was chosen for security implementation due to its increased strength. Chaos was generated through semiconductor lasers, where parameters were controlled for desired bandwidth and amplitude. EEG signals modulated through CW laser light was mixed with this chaos and transmitted over the single mode optical fiber. The properties of chaos hiding EEG signal was evaluated for long distance communication. Three different lengths i.e., 5 km, 80 km and 120 km were selected for this purpose. Linear impairments i.e., dispersion and attenuation were controlled by using optical amplifier and DCF respectively for successful propagation of EEG signal. Frequency and time domain analysis of the propagated signal confirmed the implementation of security features in EEG signal. At the receiving side, optical subtractor was used to separate EEG signals from chaos. Our results show that after 120 km of fiber length the Q-factor of the received signal drastically reduced to 5.72 which was 66.67 at 5 km fiber length.

REFERENCES

[1] S. M. Anwar, S. M. U. Saeed, M. Majid, S. Usman, C. A. Mehmood, and W. Liu, "A game player expertise level classification system using electroencephalography (EEG)," *Appl. Sci.*, vol. 8, no. 1, p. 18, 2018.

[2] D. P. Subha, P. K. Joseph, R. Acharya, and C. M. Lim, "EEG signal analysis: A survey," *J. Med. Syst.*, vol. 34, no. 2, pp. 195–212, 2010.

[3] R. Mukherjee, S. S. Dhar, and K. Tara, "Prediction of disorder of brain using EEG signal processing in MATLAB GUI platform," in *Proc. 2nd Int. Conf. Elect. Electron. Eng. (ICEEE)*, Dec. 2017, pp. 1–4.

[4] A. Raheel, S. M. Anwar, and M. Majid, "Emotion recognition in response to traditional and tactile enhanced multimedia using electroencephalography," *Multimedia Tools Appl.*, pp. 1–15, Nov. 2018.

[5] S. M. Umar, S. M. Anwar, M. Majid, M. Awais, and M. Alnowami, "Selection of neural oscillatory features for human stress classification with single channel eeg headset," *BioMed Res. Int.*, vol. 2018, Dec. 2018, Art. no. 1049257.

[6] A. Mehreen, S. M. Anwar, M. Haseeb, M. Majid, and M. O. Ullah, "A hybrid scheme for drowsiness detection using wearable sensors," *IEEE Sensors J.*, to be published.

[7] T. Hayajneh, B. J. Mohd, M. Imran, G. Almashaqbeh, and A. V. Vasilakos, "Secure authentication for remote patient monitoring with wireless medical sensor networks," *Sensors*, vol. 16, no. 4, p. 424, 2016.

[8] P. D. Healy, R. D. O'Reilly, G. B. Boylan, and J. P. Morrison, "Web-based remote monitoring of live EEG," in *Proc. 12th IEEE Int. Conf. e-Health Netw. Appl. Services (Healthcom)*, Jul. 2010, pp. 169–174.

[9] S. C. Gupta, *Textbook on Optical Fiber Communication and Its Applications*. New Delhi, India: PHI Learning, 2018.

[10] C. Zhang, W. Zhang, X. He, C. Chen, H. Zhang, and K. Qiu, "Physically secured optical OFDM-PON by employing chaotic pseudorandom RF subcarriers," *IEEE Photon. J.*, vol. 9, no. 5, Oct. 2017, Art. no. 7204408.

[11] W. Zhang, C. Zhang, C. Chen, and K. Qiu, "Experimental demonstration of security-enhanced OFDMA-PON using chaotic constellation transformation and pilot-aided secure key agreement," *J. Lightw. Technol.*, vol. 35, no. 9, pp. 1524–1530, May 1, 2017.

[12] C. Zhang, W. Zhang, C. Chen, X. He, and K. Qiu, "Physical-enhanced secure strategy for OFDMA-PON using chaos and deoxyribonucleic acid encoding," *J. Lightw. Technol.*, vol. 36, no. 9, pp. 1706–1712, May 1, 2018.

[13] T. Wu *et al.*, "Security enhancement for OFDM-PON using Brownian motion and chaos in cell," *Opt. Express*, vol. 26, no. 18, pp. 22857–22865, Sep. 2018.

[14] J. Ai, L. Wang, and J. Wang, "Secure communications of CAP-4 and OOK signals over MMF based on electro-optic chaos," *Opt. Lett.*, vol. 42, no. 18, pp. 3662–3665, Sep. 2017.

[15] N. Jiang, A. Zhao, S. Liu, C. Xue, and K. Qiu, "One physical-enhanced security strategy for all-optical chaos communication based on semiconductor lasers," *Proc. SPIE*, vol. 10812, Nov. 2018, Art. no. 108120A.

[16] L. Zhang *et al.*, "640-Gbit/s fast physical random number generation using a broadband chaotic semiconductor laser," *Sci. Rep.*, vol. 7, Apr. 2017, Art. no. 45900.

[17] W. Tian, L. Zhang, J. Ding, S. Shao, X. Fu, and L. Yang, "Ultrafast physical random bit generation from a chaotic oscillator with a silicon modulator," *Opt. Lett.*, vol. 43, no. 2, pp. 4839–4842, 2018.

[18] N. Jiang, C. Wang, C. Xue, G. Li, S. Lin, and K. Qiu, "Generation of flat wideband chaos with suppressed time delay signature by using optical time lens," *Opt. Express*, vol. 25, no. 2, pp. 14359–14367, 2017.

[19] M.-J. Zhang *et al.*, "Photonic ultrawideband signal generator using an optically injected chaotic semiconductor laser," *Opt. Lett.*, vol. 36, no. 6, pp. 1008–1010, Mar. 2011.

[20] C.-H. Cheng, C.-Y. Chen, J.-D. Chen, D.-K. Pan, K.-T. Ting, and F.-Y. Lin, "3D pulsed chaos LiDAR system," *Opt. Express*, vol. 26, no. 9, pp. 12230–12241, Apr. 2018.

[21] C.-Y. Chen, C.-H. Cheng, D.-K. Pan, and F.-Y. Lin, "Experimental generation and analysis of chaos-modulated pulses for pulsed chaos lidar applications based on gain-switched semiconductor lasers subject to optical feedback," *Opt. Express*, vol. 26, no. 16, pp. 20851–20860, 2018.

[22] L. Zhang, B. Pan, G. Chen, D. Lu, and L. Zhao, "Long-range and high-resolution correlation optical time-domain reflectometry using a monolithic integrated broadband chaotic laser," *Appl. Opt.*, vol. 56, no. 2, pp. 1253–1256, 2017.

[23] X. Dong *et al.*, "Combined attenuation and high-resolution fault measurements using chaos-OTDR," *IEEE Photon. J.*, vol. 7, no. 6, Dec. 2015, Art. no. 6804006.

[24] M. Zhang, Y. Ji, Y. Zhang, Y. Wu, H. Xu, and W. Xu, "Remote radar based on chaos generation and radio over fiber," *IEEE Photon. J.*, vol. 6, no. 5, Oct. 2014, Art. no. 7902412.

[25] M. Zhang, A. Wang, and Y. Wang, "Chaotic light generation and its application in communication, sensor, radar," in *Proc. 14th Int. Conf. Opt. Commun. Netw. (ICOCN)*, Jul. 2015, pp. 1–3.

[26] M. Preishuber, T. Hütter, S. Katzenbeisser, and A. Uhl, "Depreciating motivation and empirical security analysis of chaos-based image and video encryption," *IEEE Trans. Inf. Forensics Security*, vol. 13, no. 9, pp. 2137–2150, Sep. 2018.

[27] P. Ping, J. Fan, Y. Mao, F. Xu, and J. Gao, "A chaos based image encryption scheme using digit-level permutation and block diffusion," *IEEE Access*, vol. 6, pp. 67581–67593, 2018.

[28] J. Ke, L. Yi, G. Xia, and W. Hu, "Chaotic optical communications over 100-km fiber transmission at 30-Gb/s bit rate," *Opt. Lett.*, vol. 43, no. 6, pp. 1323–1326, Mar. 2018.

[29] N. X. Quyen and K. Kyamakya, "Chaos-based digital communication systems with low data-rate wireless applications," in *Recent Advances in Nonlinear Dynamics and Synchronization*. Cham, Switzerland: Springer, 2018, pp. 239–269.

[30] A. Niaz, F. Qamar, M. Ali, R. Farhan, and M. K. Islam, "Performance analysis of chaotic FSO communication system under different weather conditions," *Trans. Emerg. Telecommun. Technol.*, vol. 30, no. 2, p. e3486, 2019.

[31] B. Naderi and H. Kheiri, "Exponential synchronization of chaotic system and application in secure communication," *Optik*, vol. 127, no. 5, pp. 2407–2412, 2016.

[32] F. Qamar, M. K. Islam, S. Z. A. Shah, R. Farhan, and M. Ali, "Secure duobinary signal transmission in optical communication networks for high performance & reliability," *IEEE Access*, vol. 5, pp. 17795–17802, 2017.

[33] S. Z. Ali, M. K. Islam, and M. Zafrullah, "Comparative analysis of chaotic properties of optical chaos generators," *Optik*, vol. 123, no. 2, pp. 950–955, 2012.

[34] S. Z. Ali, M. K. Islam, and M. Zafrullah, "Effect of parametric variation on generation and enhancement of chaos in erbium-doped fiber-ring lasers," *Opt. Eng.*, vol. 49, no. 10, 2010, Art. no. 05002.

[35] R. Vicente, J. Daudén, P. Colet, and R. Toral, "Analysis and characterization of the hyperchaos generated by a semiconductor laser subject to a delayed feedback loop," *IEEE J. Quantum Electron.*, vol. 41, no. 4, pp. 541–548, Apr. 2005.
[36] F. Qamar *et al.*, "Secure optical QAM transmission using chaos message masking," *J. Opt. Commun.*, May 2019. doi: 10.1515/joc-2018-0225.
[37] N. Takahiro, *Fundamentals of Semiconductor Lasers*. Tokyo, Japan: Springer, 2015, pp. 89–186.
[38] W. Zhang, C. Zhang, C. Chen, H. Zhang, W. Jin, and K. Qiu, "Hybrid chaotic confusion and diffusion for physical layer security in OFDM-PON," *IEEE Photon. J.*, vol. 9, no. 2, Apr. 2017, Art. no. 7201010.
[39] W. Zhang, C. Zhang, C. Chen, H. Zhang, and K. Qiu, "Brownian motion encryption for physical-layer security improvement in CO-OFDM-PON," *IEEE Photon. Technol. Lett.*, vol. 29, no. 12, pp. 1023–1026, Jun. 15, 2017.

ROMANA SHAHZADI received the B.Sc.Engg. and M.Sc.Engg. degrees (Hons.) in computer engineering from the University of Engineering and Technology (UET), Taxila, Pakistan, in 2008 and 2011, respectively. She is currently pursuing the Ph.D. degree with the Department of Computer Engineering, UET. Her research interests include data, networks, and system security with a focus on e-health systems.

SYED MUHAMMAD ANWAR received the B.Sc. degree (Hons.) in computer engineering from the University of Engineering and Technology (UET), Taxila, Pakistan, in 2005, the M.Sc. degree (Hons.) in data communications and the Ph.D. degree in electronic and electrical engineering from the University of Sheffield, U.K., in 2007 and 2012, respectively. He is currently an Associate Professor with the Department of Software Engineering, UET, and he has been the Head of the Signal, Image, Multimedia Processing and Learning (SIMPLE) Research Group, since 2012. He was a recipient of the Faculty Development Program Scholarship of Higher Education Commission (HEC), Pakistan, for the M.Sc. and Ph.D. degrees. His research interests include biomedical signal processing, medical imaging, physiological signal processing, and deep learning.

FARHAN QAMAR received the B.Sc. degree in computer engineering, the M.Sc. degree in telecommunication engineering, and the Ph.D. degree in telecommunication engineering from the University of Engineering and Technology, Taxila, Pakistan. After his graduation, he remained attached with different sections of Huawei and Mobilink for over seven years. For the last six years, he was an Assistant Professor with the Telecom Engineering Department, University of Engineering and Technology, Taxila, where he is also acting as a Principal Investigator of the Advance Optical Communication Group (AOCG). His areas of interest include chaos communication, optical networks, 5G networks, advance modulation formats, and radio over fiber.

MUDASSAR ALI received the B.S. degree in computer engineering and the M.S. degree in telecom engineering from the University of Engineering and Technology, Taxila, Pakistan, in 2006 and 2010, respectively, with a major in wireless communication, and the Ph.D. degree from the School of Electrical Engineering and Computer Science (SEECS), National University of Sciences and Technology (NUST), Pakistan, in 2017. From 2006 to 2007, he was a Network Performance Engineer with Mobilink (An Orascom Telecom Company). From 2008 to 2012, he was a Senior Engineer in radio access network optimization with Zong (A China Mobile Company). Since 2012, he has been an Assistant Professor with the Telecom Engineering Department, UET, Taxila. His research interests include 5G wireless systems, heterogeneous networks, interference coordination, and energy efficiency in 5G green heterogeneous networks.

JOEL J. P. C. RODRIGUES (S'01–M'06–SM'06) received the B.Sc. degree (licentiate) in informatics engineering from the University of Coimbra, Portugal, the Habilitation degree in computer science and engineering from the University of Haute Alsace, France, the M.Sc. degree from the University of Beira Interior, and the Ph.D. degree in informatics engineering. He is currently a Professor with the Department of Informatics, University of Beira Interior, Covilha, Portugal, and a Researcher with the Instituto de Telecomunicações, Portugal. His main research interests include sensor networks, e-health, e-learning, vehicular delay tolerant networks, and mobile and ubiquitous computing. He is a Licensed Professional Engineer (as Senior Member), a member of the Internet Society, an IARIA Fellow, and a Senior Member of the IT and ACM. He is a Leader of the NetGNA Research Group, the Chair of the IEEE ComSoc Technical Committee on eHealth, and the Past-Chair of the IEEE ComSoc Technical Committee on Communications Software. He is a Steering Committee member of the IEEE Life Sciences Technical Community, a Member Representative of the IEEE Communications Society, IEEE Biometrics Council, and an Officer of the IEEE 1907.1 Standard. He has been the General Chair and the TPC Chair of many international conferences, including the IEEE ICC and GLOBECOM. He is a member of many international TPCs, and he has participated in several international conferences organization. He has authored or coauthored over 400 papers in refereed international journals and conferences. He holds a book and three patents. He has received several Outstanding Leadership and Outstanding Service Awards from the IEEE Communications Society and several Best Paper Awards. He is the Editor-in-Chief of the *International Journal on E-Health and Medical Communications*, the *Recent Advances on Communications and Networking Technology*, and *The Journal of Multimedia Information Systems*. He is Editorial Board Member of several journals.

MAJDI ALNOWAMI received the Ph.D. degree in medical physics from the University of Surrey. He is currently working as an Assistant Professor in King Abdulaziz University, and he has authored several peer-reviewed articles in leading conferences and journals. His research interests include medical imaging, treatment planning, and biomedical signal processing.